Arch. Mech., **51**, 3–4, pp. 335–355, Warszawa 1999

Application of homogenization to evaluation of effective moduli of linear elastic trabecular bone with plate-like structure

A. GAŁKA, J.J. TELEGA and S. TOKARZEWSKI

Polish Academy of Sciences
Institute of Fundamental Technological Research
Świętokrzyska 00–049 Warszawa, Poland
e-mail: jtelega@ippt.gov.pl

CANCELLOUS BONE with plate-like architecture is modelled as an elastic cellular solid with regular microstructure. General formulae for the effective moduli are derived. Specific examples concern plate-like cancellous bone with isotropic trabeculae.

1. Introduction

BONES OCCUR IN TWO FORMS: as a dense solid *(compact bone)* and as a porous network of interconnected rods and plates *(cancellous or trabecular bone)*. The most obvious difference between these two types of bones appears in their relative densities measured by volume fractions of solids, cf. Fig 1.

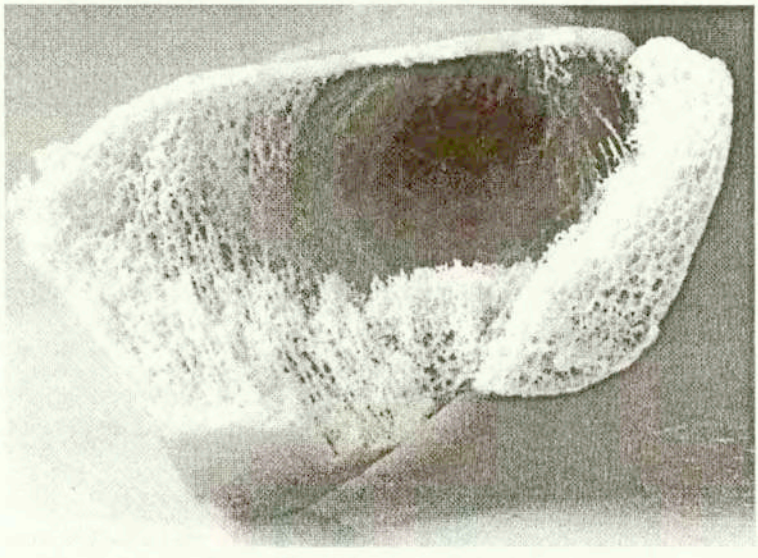

FIG. 1. Photograph of proximal part of the human femur.

Bone with a volume fraction of less than 70% is classified as cancellous while that over 70% is compact, cf. [13]. Most bones in the body are of both types, the dense compact bone forming an outer shell surrounding a core of spongy cancellous bone. This paper investigates cancellous bones of volume fractions of solid less than 70%. Typical examples of trabecular bones are shown in Figs. 2–4.

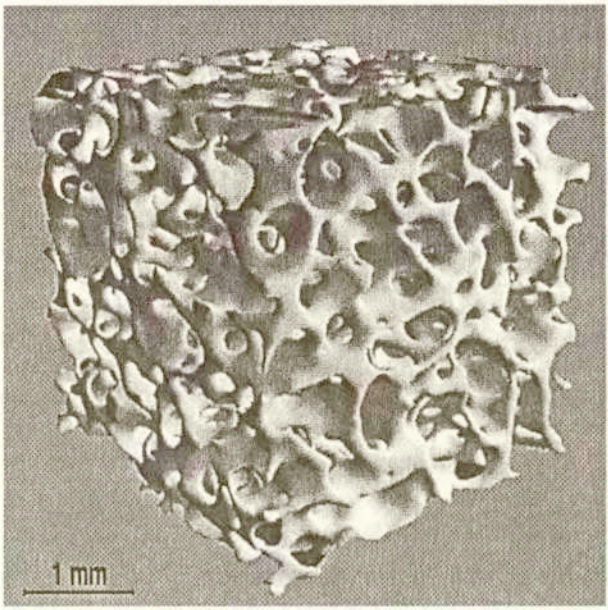

FIG. 2. Micro-CT image of a trabecular bone specimen with rod-like architecture and a bone volume fraction of 26%, after [33].

These figures provide interesting visualization of human trabecular bone architecture obtained by micro-computed tomography [24, 33]. According to MÜLLER and RÜEGSEGGER [24], specimens with diameters of a few millimeters to a maximum of 18 mm can be measured. Microstructure analyses of trabecular bone have followed the general approach used in the cellular plastics fields. MCELHANEY *et al.* [22] developed a porous block model of trabecular bone based on integration of spring stiffness loaded in parallel or in series. Using this model, they found good agreement between the prediction of apparent stiffness and the experimentally measured stiffness values in some internal layer of human skull. PUGH *et al.* [27] modelled the subchondral trabecular bone as a collection of structural plates and concluded that bending and buckling were major modes of deformation of the trabecular bone. WILLIAMS and LEWIS [34] modelled the exact structure of a two-dimensional section of trabecular bone with plane strain finite elements to predict the apparent transversely isotropic elastic constants. GIBSON [12] developed the models of trabecular bone structure using analytical

FIG. 3. Trabecular bone with distinct rod-like columnar structure, after [24].

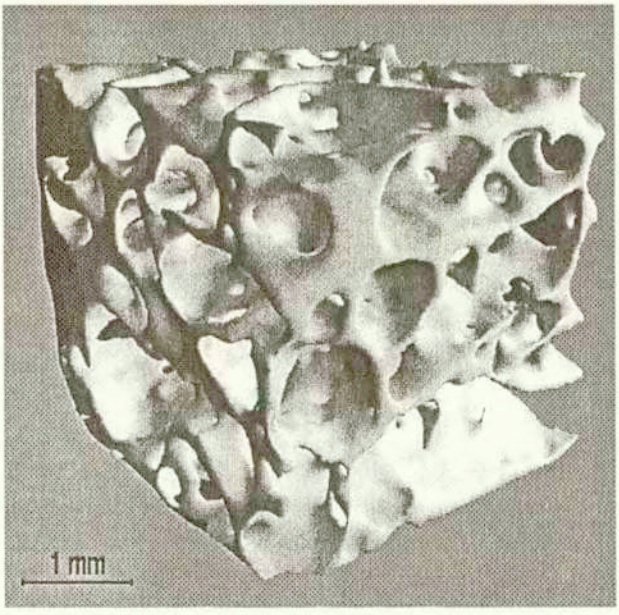

FIG. 4. Micro-CT image of a trabecular bone specimen with plate-like architecture and a bone volume fraction of 26%, after [33].

techniques for porous solids. He predicted the dependence of apparent stiffness on apparent density for different structural types of trabecular bones. BEAUPRÉ and HAYES [3] developed a three-dimensional spherical void model of trabecular bone and used finite element analyses to predict apparent stiffness and strength, as well the stress distribution within the trabecular bone. HOLLISTER *et al.* [14, 15] applied the homogenization theory [6, 19, 28, 29] for an investigation of mechanical behaviour of rod-like structures modelling the trabecular bones. By using the finite element method they evaluated the apparent, orthogonal Young's moduli and compared them with the experimental data obtained for proximal humerus, proximal tibia and distal femur. Bone may be viewed as a structurally hierarchical porous material. It is then possible to use the iterative homogenization [6] to derive the formulae for the macroscopic elastic moduli, cf. [1, 2, 10, 11]. Optimal design of structures often involves the homogenization and relaxation methods [4, 5, 18, 19, 21, 30]. Such an approach may be used to model bone microstructure via adaptive elasticity. PAYTEN *et al.* [26] presented an optimisation process that has, as its basis, an algorithm originally developed for predicting anatomical density distributions in natural human bones.

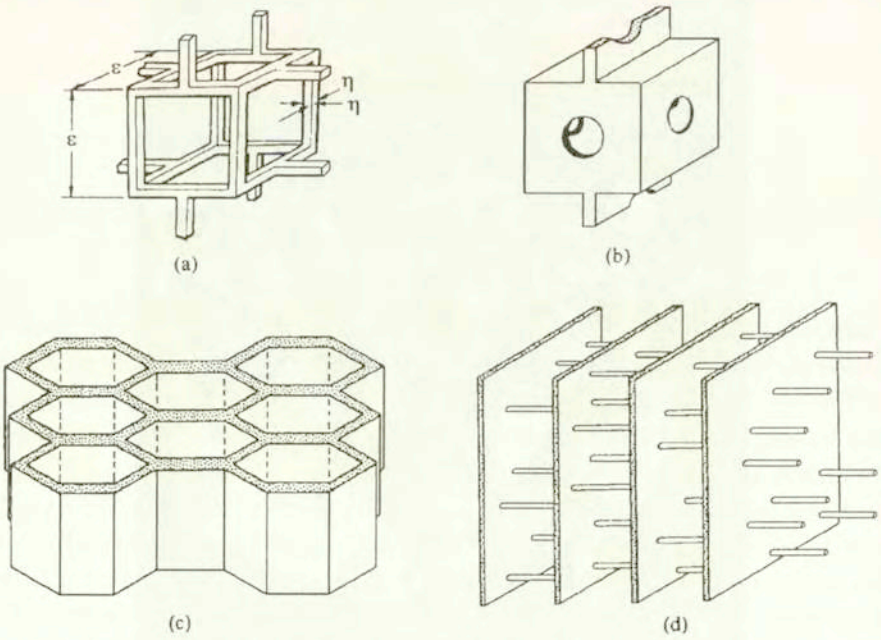

FIG. 5. Models for the structure of cancellous bone: (a) the low-density equiaxed structure, (b) the higher-density equiaxial structure, (c) the stress-oriented prismatic structure and (d) the stress-oriented parallel plate structure, after [13].

The microstructure of bone is such that at the macroscopic level its behaviour is anisotropic. To model bone anisotropy one can use Cowin's fabric tensor,

see [9, 16, 20] and the references cited therein. JEMIOŁO and TELEGA [16] prove that compact bone is close to transverse isotropy whilst trabecular bone is approximately orthotropic, cf. also [35]. The approach employed in [16] exploits Cowin's fabric tensor. In [35] the authors claim to use the homogenization method for finding the orthotropic elastic constants, yet no precise formulation was unfortunately given.

A challenging problem in the estimation of bone elastic moduli is the influence of marrow. No satisfactory modelling of this problem seems to have been proposed so far. KASRA and GRYNPAS [17] proposed an idealized three-dimensional finite element model of a rod-like trabecular bone structure to study its static and dynamic response under compressive loading. Static analysis of the model predicted hydraulic stiffening of trabecular bone due to the presence of bone narrow. The predicted power equation relating the trabecular bone apparent elastic modulus to its apparent density was in good agreement with those of the reported experimental data.

The aim of this paper is to develop a macroscopic model of cancellous bone by using the homogenization methods. In contrast to numerical considerations adopted in [14, 15] for the study of strut-like trabecular bone, our approach applies to plate-like architecture of cancellous bone and was inspired by the papers [7, 8]. General considerations are performed in Secs. 2 and 3 and extend those obtained in [7], where only the scalar case was investigated. In fact, the homogenization problem considered involved two small positive parameters: ε and η. The first parameter is standard in the homogenization whilst the second one characterizes the thickness of the trabecular plates. To derive the formula for the elastic macroscopic moduli, we first pass with ε to zero and next we let η tend to zero. It means that a two-parameter homogenization has been performed. Section 4 deals with a specific case of trabecular bone with plate-like structure, where the trabecular plates are isotropic. By properly choosing the geometry of the basic cell one can model anisotropic (orthotropic or transversely isotropic) behaviour of the cancellous bone at the macroscopic level. If $\alpha = \beta = 1$, at the macroscopic level the bone reveals the cubic symmetry, cf. formula (4.1).

2. Formulation of the problem

Let Ω denote a bounded open subset of $\mathbb{R}^3$. As usual by Y we denote the basic cell, cf. [6, 19, 28, 29]. The part of Y occupied by the material is denoted by Y^*. It is assumed that the hole T in Y does not intersect the boundary ∂Y, cf. [7, 19], though this assumption may be weakened. By Ω_ε^* we denote the part of Ω occupied by the material. Here $\varepsilon > 0$ is a small parameter. We asume that the holes do not meet the boundary $\partial\Omega$.

Let us consider the following boundary value problem of linear elasticity:

$$\frac{\partial}{\partial x_j}\left(C_{ijkl}\left(\frac{\mathbf{x}}{\varepsilon}\right)\frac{\partial u_k^\varepsilon}{\partial x_l}\right)+f_i=0 \quad \text{in } \Omega_\varepsilon^*,$$

$$u_k^\varepsilon = 0 \quad \text{on } \partial\Omega, \tag{2.1}$$

$$C_{ijkl}\left(\frac{\mathbf{x}}{\varepsilon}\right)\frac{\partial u_k^\varepsilon}{\partial x_l}n_j = 0 \quad \text{on } \partial\Omega_\varepsilon^*\backslash\partial\Omega,$$

where $\mathbf{n}=(n_j)$ is outer the unit vector normal to $\partial\Omega_\varepsilon^*\backslash\partial\Omega$.

We make the following assumptions:

(i) $f\in L^2(\Omega)$.

(ii) $C_{ijkl}\in L^\infty(Y^*)$, $C_{ijkl}=C_{klij}=C_{jikl}$, $i,j,k,l=1,2,3$.

(iii) There exist a positive constant c_0 such that for almost every $\mathbf{y}\in Y$:

$$C_{ijkl}(\mathbf{y})e_{ij}e_{kl}\geqslant C_0 e_{ij}e_{ij} \quad \text{for any} \quad \mathbf{e}=(e_{ij}),\ e_{ij}=e_{ji}.$$

(iv) The material coefficients $C_{ijkl}(\mathbf{y})$ are Y-periodic.

The passage with ε to zero is now standard. Let us recall the related basic results which will next be exploited in Sec. 3, where we will let η tend to zero. Under these assumptions, there exists an extension $P_\varepsilon\mathbf{u}^\varepsilon\in\left[H_0^1(\Omega)\right]^3$ of $\mathbf{u}^\varepsilon$ such that, cf. [7, 19],

$$P_\varepsilon\mathbf{u}^\varepsilon \rightharpoonup \mathbf{u} \quad \text{in } \left[H_0^1(\Omega)\right]^3 \text{ weakly},$$

with $\mathbf{u}=(u_k)$ being the solution of the equation

$$C_{ijkl}^h\frac{\partial^2 u_k}{\partial x_j\partial x_l}+\frac{|Y^*|}{|Y|}f_i=0 \quad \text{in } \Omega, \tag{2.2}$$

$$\mathbf{u}=\mathbf{0}, \quad \text{on } \partial\Omega.$$

Here $|Y|=vol\ Y$.

The homogenized coefficient C_{ijkl}^h are given by

$$C_{ijmn}^h = < C_{ijmn} > + < C_{ijpq}\frac{\partial\chi_p^{(mn)}}{\partial y_q} >, \tag{2.3}$$

where

$$< \cdot >= \frac{1}{|Y|}\int_{Y^*}(\cdot)d\mathbf{y}. \tag{2.4}$$

The Y-periodic functions $\chi_p^{(mn)}$ are solutions to the local problem

$$\frac{\partial}{\partial y_i}\left(C_{ijmn}\frac{\partial}{\partial y_n}\left(\chi_m^{(pq)}+\delta_m^p y^q\right)\right)=0 \quad \text{in } Y^*, \tag{2.5}$$

$$C_{ijmn}\frac{\partial}{\partial y_n}\left(\chi_m^{(pq)}+\delta_m^p y^q\right)N_i=0 \quad \text{on } \partial T. \tag{2.6}$$

Here $\mathbf{N}$ stands for the inner unit vector normal to ∂T. Written in the weak form, this problem is expressed by

$$\int\limits_{Y^*} C_{ijmn}\frac{\partial\chi_m^{(pq)}}{\partial y_n}\frac{\partial\Psi_j}{\partial y_i}\,d\mathbf{y}=-\int\limits_{Y^*} C_{ijpq}\frac{\partial\Psi_j}{\partial y_i}\,d\mathbf{y}, \qquad \forall\,\Psi_j\in H_{\mathrm{per}}(Y^*), \tag{2.7}$$

where

$$H_{\mathrm{per}}(Y^*)=\left\{v\in H^1(Y^*)\mid v \text{ is } Y-\text{periodic}\right\}.$$

For $\Psi_j=\chi_j^{(mn)}$ we get

$$\int\limits_{Y^*} C_{ijmn}\frac{\partial\chi_m^{(pq)}}{\partial y_n}\frac{\partial\chi_j^{(mn)}}{\partial y_i}\,d\mathbf{y}=-\int\limits_{Y^*} C_{ijpq}\frac{\partial\chi_j^{(mn)}}{\partial y_i}\,d\mathbf{y}. \tag{2.8}$$

3. Plate-like structure

In this section we shall derive the macroscopic moduli for a cellular solid with plate-like architecture. The plates are characterized by a small parameter $\eta>0$. The second step of homogenization consists in passing with η to zero. Let now the basic cell Y be given by

$$Y=\left[-\frac{1}{2},\frac{1}{2}\right)\times\left[-\frac{1}{2},\frac{1}{2}\right)\times\left[-\frac{1}{2},\frac{1}{2}\right). \tag{3.1}$$

Due to periodicity, the homogenized coefficients do not depend on the basic cell and consequently, one may take a translated cell of the basic one. Consequently we take the translated cell represented in Fig. 6.

We observe that the thicknesses of three orthogonal plates are not necessarily equal, thus allowing for a macroscopically orthotropic response of the trabecular bone. Let us introduce the following notation:

$$\begin{aligned}
Y_1&=\left\{\mathbf{y}\in Y,|y_1|\leqslant\frac{\eta}{2}\right\},\\
Y_2&=\left\{\mathbf{y}\in Y,|y_2|\leqslant\alpha\frac{\eta}{2}\right\},\\
Y_3&=\left\{\mathbf{y}\in Y,|y_3|\leqslant\beta\frac{\eta}{2}\right\},\\
Y_{12}&=\left\{\mathbf{y}\in Y,|y_1|\leqslant\frac{\eta}{2}\text{ and }|y_2|\leqslant\alpha\frac{\eta}{2}\right\},
\end{aligned} \tag{3.2}$$

(3.2) [cont.]

$$Y_{23} = \left\{ \mathbf{y} \in Y, |y_2| \leqslant \alpha \frac{\eta}{2} \text{ and } |y_3| \leqslant \beta \frac{\eta}{2} \right\},$$

$$Y_{13} = \left\{ \mathbf{y} \in Y, |y_1| \leqslant \frac{\eta}{2} \text{ and } |y_3| \leqslant \beta \frac{\eta}{2} \right\},$$

$$Y_{123} = \left\{ \mathbf{y} \in Y, |y_1| \leqslant \frac{\eta}{2} \text{ and } |y_2| \leqslant \alpha \frac{\eta}{2} \text{ and } |y_3| \leqslant \beta \frac{\eta}{2} \right\},$$

$$Y_\eta^* = \left\{ \mathbf{y} \in Y, |y_1| \leqslant \frac{\eta}{2} \text{ or } |y_2| \leqslant \alpha \frac{\eta}{2} \text{ or } |y_3| \leqslant \beta \frac{\eta}{2} \right\}.$$

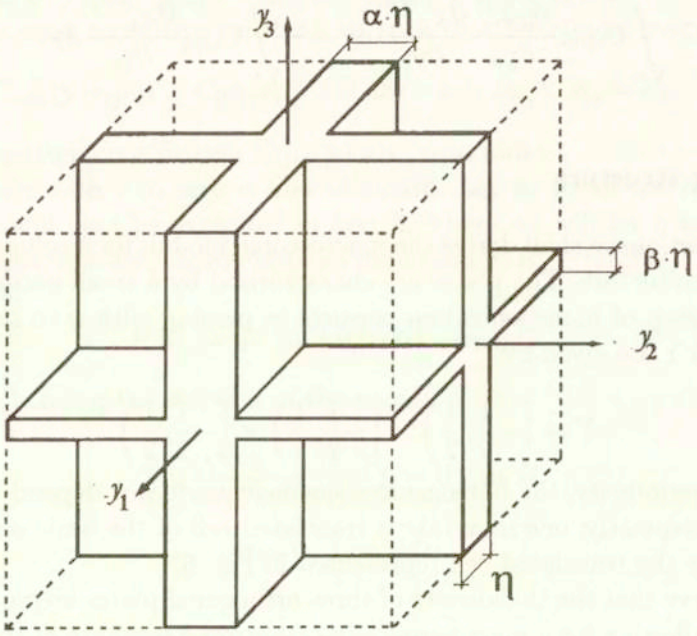

FIG. 6.

We follow the paper [7], where only two-dimensional scalar case was examined. Since $|Y_\eta^*| = (1+\alpha+\beta)\,\eta - (\alpha+\beta+\alpha\,\beta)\,\eta^2 + \alpha\,\beta\,\eta^3$, we get the following estimate:

$$||\mathbf{e}^y(\boldsymbol{\chi}^{(pq)})||_{L^2(Y_\eta^*)} \leqslant c\,\eta^{1/2}. \tag{3.3}$$

Obviously $\boldsymbol{\chi}^{(pq)}$ depend on α, β and η. The constant c is independent of η and

$$e^y(\mathbf{w}) = \frac{1}{2}\left(\frac{\partial w_i}{\partial y_j} + \frac{\partial w_j}{\partial y_i}\right).$$

Using this estimate in (2.3) we conclude that

$$\eta^{-1} C^h_{ijmn} \to C^*_{ijmn}$$

(after extraction of a subsequence, if necessary) We can pass to the limit as $\eta \to 0$ in the homogenized equation (2.2), whose solution is denoted by $\mathbf{u}^\eta$. We have

$$u^\eta_k \rightharpoonup u^*_k \quad \text{in} \quad H^1_0(\Omega) \text{ weakly},$$

where $\mathbf{u}^*$ is the solution to the equation:

$$C^*_{ijkn} \frac{\partial^2 u^*_k}{\partial x_j \partial x_n} + (1 + \alpha + \beta) f_i = 0 \quad \text{in} \quad \Omega, \tag{3.4}$$

$$\mathbf{u}^* = 0 \quad \text{on} \quad \partial\Omega.$$

We observe that now $|Y| = 1$.

Let us pass to finding the limit coefficients C^*_{ijkn}.

Using Eq. (2.3) and the decomposition of Y^* given by (3.2), we obtain:

$$\begin{aligned} \eta^{-1} C^h_{ijmn} = \eta^{-1} |Y^*| C_{ijmn} - \eta^{-1} \int\limits_{Y_1} C_{ijpq} \frac{\partial \chi^{(mn)}_p}{\partial y_q} \, d\mathbf{y} \\ - \eta^{-1} \int\limits_{Y_2} C_{ijpq} \frac{\partial \chi^{(mn)}_p}{\partial y_q} \, d\mathbf{y} - \eta^{-1} \int\limits_{Y_3} C_{ijpq} \frac{\partial \chi^{(mn)}_p}{\partial y_q} \, d\mathbf{y} \\ + \eta^{-1} \int\limits_{Y_{12}} C_{ijpq} \frac{\partial \chi^{(mn)}_p}{\partial y_q} \, d\mathbf{y} + \eta^{-1} \int\limits_{Y_{23}} C_{ijpq} \frac{\partial \chi^{(mn)}_p}{\partial y_q} \, d\mathbf{y} \\ + \eta^{-1} \int\limits_{Y_{13}} C_{ijpq} \frac{\partial \chi^{(mn)}_p}{\partial y_q} \, d\mathbf{y} - \eta^{-1} \int\limits_{Y_{123}} C_{ijpq} \frac{\partial \chi^{(mn)}_p}{\partial y_q} \, d\mathbf{y}. \end{aligned} \tag{3.5}$$

We have to pass to the limit with $\eta \to 0$ in (3.5), where the integral terms are taken over domains depending on η. To avoid this difficulty we transform Y_1, Y_2, Y_3, Y_{12}, Y_{23}, Y_{13} and Y_{123} in $\overline{Y}$.

For instance, using the a priori estimate (3.3) we have

$$\int\limits_{Y_1} \left| \mathbf{e}^y \left(\chi^{(pq)} \right) \right| \, d\mathbf{y} \leqslant c\eta.$$

Hence, after transformation

$$z_1 = \eta^{-1} y_1, \; z_2 = y_2, \; z_3 = y_3,$$

and using Korn's inequality we get

$$\int\limits_Y \left[\left(\eta^{-1} \frac{\partial \chi_{p1}^{(mn)}}{\partial z_1} \right)^2 + \left(\frac{\partial \chi_{p1}^{(mn)}}{\partial z_2} \right)^2 + \left(\frac{\partial \chi_{p1}^{(mn)}}{\partial z_3} \right)^2 \right] d\mathbf{z} \leqslant c_1,$$

where $\chi_{p1}^{(mn)} = \chi_{p1}^{(mn)}(z_1, z_2, z_3) = \chi_p^{(mn)}(\eta z_1, z_2, z_3)$ and c_1 does not depend on η.

Thus

$$\eta^{-1} \frac{\partial \chi_{p1}^{(mn)}}{\partial z_1} \rightharpoonup h_{p1,1}^{(mn)}, \quad \frac{\partial \chi_{p1}^{(mn)}}{\partial z_2} \rightharpoonup h_{p1,2}^{(mn)}, \quad \frac{\partial \chi_{p1}^{(mn)}}{\partial z_3} \rightharpoonup h_{p1,3}^{(mn)}, \tag{3.6}$$

in $L^2(Y)$ weakly

and similarly

$$\frac{\partial \chi_{p2}^{(mn)}}{\partial z_1} \rightharpoonup h_{p2,1}^{(mn)}, \quad \eta^{-1} \frac{\partial \chi_{p2}^{(mn)}}{\partial z_2} \rightharpoonup h_{p2,2}^{(mn)}, \quad \frac{\partial \chi_{p2}^{(mn)}}{\partial z_3} \rightharpoonup h_{p2,3}^{(mn)},$$

in $L^2(Y)$ weakly,

$$\frac{\partial \chi_{p3}^{(mn)}}{\partial z_1} \rightharpoonup h_{p3,1}^{(mn)}, \quad \frac{\partial \chi_{p3}^{(mn)}}{\partial z_2} \rightharpoonup h_{p1,3}^{(mn)}, \quad \eta^{-1} \frac{\partial \chi_{p3}^{(mn)}}{\partial z_3} \rightharpoonup h_{p3,3}^{(mn)},$$

in $L^2(Y)$ weakly,

$$\eta^{-1/2} \frac{\partial \chi_{p12}^{(mn)}}{\partial z_1} \rightharpoonup h_{p12,1}^{(mn)}, \quad \eta^{-1/2} \frac{\partial \chi_{p12}^{(mn)}}{\partial z_2} \rightharpoonup h_{p12,2}^{(mn)}, \quad \frac{\partial \chi_{p12}^{(mn)}}{\partial z_3} \rightharpoonup h_{p12,3}^{(mn)},$$

in $L^2(Y)$ weakly,

(3.7)

$$\frac{\partial \chi_{p23}^{(mn)}}{\partial z_1} \rightharpoonup h_{p23,1}^{(mn)}, \quad \eta^{-1/2} \frac{\partial \chi_{p23}^{(mn)}}{\partial z_2} \rightharpoonup h_{p23,2}^{(mn)}, \quad \eta^{-1/2} \frac{\partial \chi_{p23}^{(mn)}}{\partial z_3} \rightharpoonup h_{p23,3}^{(mn)},$$

in $L^2(Y)$ weakly,

$$\eta^{-1/2} \frac{\partial \chi_{p13}^{(mn)}}{\partial z_1} \rightharpoonup h_{p13,1}^{(mn)}, \quad \frac{\partial \chi_{p13}^{(mn)}}{\partial z_2} \rightharpoonup h_{p13,2}^{(mn)}, \quad \eta^{-1/2} \frac{\partial \chi_{p13}^{(mn)}}{\partial z_3} \rightharpoonup h_{p13,3}^{(mn)},$$

in $L^2(Y)$ weakly,

$$\frac{\partial \chi_{p123}^{(mn)}}{\partial z_1} \rightharpoonup h_{p123,1}^{(mn)}, \quad \frac{\partial \chi_{p123}^{(mn)}}{\partial z_2} \rightharpoonup h_{p123,2}^{(mn)}, \quad \frac{\partial \chi_{p123}^{(mn)}}{\partial z_3} \rightharpoonup h_{p123,3}^{(mn)},$$

in $L^2(Y)$ weakly.

Here

$$\chi_{p2}^{(mn)} = \chi_{p2}^{(mn)}(z_1, z_2, z_3) = \chi_p^{(mn)}(z_1, \alpha\eta z_2, z_3),$$

$$\chi_{p3}^{(mn)} = \chi_{p3}^{(mn)}(z_1, z_2, z_3) = \chi_p^{(mn)}(z_1, z_2, \beta\eta z_3),$$

$$\chi_{p12}^{(mn)} = \chi_{p12}^{(mn)}(z_1, z_2, z_3) = \chi_p^{(mn)}(\eta z_1, \alpha\eta z_2, z_3),$$

$$\chi_{p23}^{(mn)} = \chi_{p23}^{(mn)}(z_1, z_2, z_3) = \chi_p^{(mn)}(z_1, \alpha\eta z_2, \beta\eta z_3),$$

$$\chi_{p13}^{(mn)} = \chi_{p13}^{(mn)}(z_1, z_2, z_3) = \chi_p^{(mn)}(\eta z_1, z_2, \beta\eta z_3),$$

$$\chi_{p123}^{(mn)} = \chi_{p123}^{(mn)}(z_1, z_2, z_3) = \chi_p^{(mn)}(\eta z_1, \alpha\eta z_2, \beta\eta z_3).$$

We observe that due to the periodicity of $\chi_p^{(mn)}$ one has:

$$\int_Y h_{p1,2}^{(mn)}\, d\mathbf{z} = 0, \quad \int_Y h_{p1,3}^{(mn)}\, d\mathbf{z} = 0, \quad \int_Y h_{p2,1}^{(mn)}\, d\mathbf{z} = 0,$$

$$\int_Y h_{p2,3}^{(mn)}\, d\mathbf{z} = 0, \quad \int_Y h_{p3,1}^{(mn)}\, d\mathbf{z} = 0, \quad \int_Y h_{p3,2}^{(mn)}\, d\mathbf{z} = 0, \tag{3.8}$$

$$\int_Y h_{p12,3}^{(mn)}\, d\mathbf{z} = 0, \quad \int_Y h_{p23,1}^{(mn)}\, d\mathbf{z} = 0, \quad \int_Y h_{p13,2}^{(mn)}\, d\mathbf{z} = 0.$$

By using (3.3) one finds

$$\left| \eta^{-1} \int_{Y_{12}} C_{ijpq} \frac{\partial \chi_p^{(mn)}}{\partial y_q}\, d\mathbf{y} \right| \leqslant c_1 \eta^{1/2}, \quad \left| \eta^{-1} \int_{Y_{23}} C_{ijpq} \frac{\partial \chi_p^{(mn)}}{\partial y_q}\, d\mathbf{y} \right| \leqslant c_1 \eta^{1/2},$$

$$\left| \eta^{-1} \int_{Y_{13}} C_{ijpq} \frac{\partial \chi_p^{(mn)}}{\partial y_q}\, d\mathbf{y} \right| \leqslant c_1 \eta^{1/2}, \quad \left| \eta^{-1} \int_{Y_{123}} C_{ijpq} \frac{\partial \chi_p^{(mn)}}{\partial y_q}\, d\mathbf{y} \right| \leqslant c_1 \eta.$$

We now pass to the limit in (3.5). Taking into account (3.6) – (3.8), one obtains:

$$C_{ijmn}^* = (1 + \alpha + \beta)\, C_{ijmn} + C_{ijp1} \int_Y h_{p1,1}^{(mn)}\, d\mathbf{z} + \alpha\, C_{ijp2} \int_Y h_{p2,2}^{(mn)}\, d\mathbf{z} + \beta\, C_{ijp3} \int_Y h_{p3,3}^{(mn)}\, d\mathbf{z}. \tag{3.9}$$

The last step is to calculate explicitly the integral terms of this formula. Let Ψ_j in (2.7) be a smooth function, Y-periodic and dependent only on y_1. We find

$$\eta^{-1} \int\limits_{Y_1} C_{1jmn} \frac{\partial \chi_m^{(pq)}}{\partial y_n} \frac{\partial \Psi_j}{\partial y_1} d\mathbf{y}$$

$$= \eta^{-1} C_{1jm1} \int\limits_{-\eta/2}^{\eta/2} \frac{\partial \Psi_j}{\partial y_1} \left(\int\limits_{-1/2}^{1/2} \int\limits_{-1/2}^{1/2} \frac{\partial \chi_m^{(pq)}}{\partial y_1} \, dy_2 \, dy_3 \right) dy_1$$

$$\to C_{1jm1} \frac{\partial \Psi_j}{\partial y_1}(0) \int\limits_Y h_{m1,1}^{(pq)} \, d\mathbf{y},$$

$$\eta^{-1} \int\limits_{Y_2} C_{1jmn} \frac{\partial \chi_m^{(pq)}}{\partial y_n} \frac{\partial \Psi_j}{\partial y_1} d\mathbf{y} \to C_{1jm1} \int\limits_Y h_{m2,1}^{(pq)} \frac{\partial \Psi_j}{\partial y_1} \, d\mathbf{y},$$

$$\eta^{-1} \int\limits_{Y_3} C_{1jmn} \frac{\partial \chi_m^{(pq)}}{\partial y_n} \frac{\partial \Psi_j}{\partial y_1} d\mathbf{y} \to C_{1jm1} \int\limits_Y h_{m3,1}^{(pq)} \frac{\partial \Psi_j}{\partial y_1} \, d\mathbf{y},$$

$$\eta^{-1} \int\limits_{Y^*} C_{1jpq} \frac{\partial \Psi_j}{\partial y_1} d\mathbf{y} \to C_{1jpq} \frac{\partial \Psi_j}{\partial y_1}(0).$$

Multiplying (2.7) by η^{-1} and passing to the limit $(\eta \to 0)$, we obtain

$$C_{1jm1} \int\limits_Y \left(h_{m2,1}^{(pq)} + h_{m3,1}^{(pq)} \right) \frac{\partial \Psi_j}{\partial y_1} \, d\mathbf{z} \tag{3.10}$$

$$+ \frac{\partial \Psi_j}{\partial y_1}(0) \left(C_{1jm1} \int\limits_Y h_{m1,1}^{(pq)} \, d\mathbf{z} + C_{1jpq} \right) = 0.$$

To proceed further we need the following result, cf. [7].

LEMMA 3.1 Let w be a periodic function in $L^2(-1/2, -1/2)$, and let a be a real constant. If the following, relation holds true:

$$a \Psi(0) + \int\limits_{-1/2}^{1/2} w(x) \Psi(x) \, dx = 0,$$

for any smooth and periodic function Ψ defined on $(-1/2, 1/2)$ and such that $\int_{-1/2}^{1/2} \Psi(x)\,dx = 0$, then

$$a = 0 \quad \text{and} \quad w = \text{ const.} \qquad \square$$

Applying this lemma to (3.10) we obtain

$$\int_Y h^{(pq)}_{m1,1} = -\left(\mathbf{C}_1^{-1}\right)_{mj} C_{1jpq},$$

where $\left(\mathbf{C}_1^{-1}\right)_{mj}$ are the components of the matrix inverse to (C_{1mj1}). Similar computation with Ψ_j depending only on y_2 leads to

$$\int_Y h^{(pq)}_{m2,2} = -\left(\mathbf{C}_2^{-1}\right)_{mj} C_{2jpq}.$$

Next, if Ψ_j depends only on y_3, then

$$\int_Y h^{(pq)}_{m3,3} = -\left(\mathbf{C}_3^{-1}\right)_{mj} C_{3jpq}.$$

Here $\left(\mathbf{C}_2^{-1}\right)_{mj}$ and $\left(\mathbf{C}_3^{-1}\right)_{mj}$ are the components of the matrices inverse to (C_{2mj2}) and (C_{3mj3}) respectively. From (3.9) we eventually obtain

$$C^*_{ijmn} = (1+\alpha+\beta)\,C_{ijmn} - C_{ijp1}\left(\mathbf{C}_1^{-1}\right)_{pq} C_{1qmn} - \alpha\, C_{ijp2}\left(\mathbf{C}_2^{-1}\right)_{pq} C_{2qmn} - \beta\, C_{ijp3}\left(\mathbf{C}_3^{-1}\right)_{pq} C_{3qmn}. \tag{3.11}$$

If we take a more general basic cell:

$$Y = \left[-\frac{1}{2}, \frac{1}{2}\right) \times \left[-\frac{A}{2}, \frac{A}{2}\right) \times \left[-\frac{B}{2}, \frac{B}{2}\right)$$

then we obtain the following formula:

$$C^*_{ijmn} = \left(1 + \frac{\alpha}{A} + \frac{\beta}{B}\right) C_{ijmn} - C_{ijp1}\left(\mathbf{C}_1^{-1}\right)_{pq} C_{1qmn} - \frac{\alpha}{A}\, C_{ijp2}\left(\mathbf{C}_2^{-1}\right)_{pq} C_{2qmn} - \frac{\beta}{B}\, C_{ijp3}\left(\mathbf{C}_3^{-1}\right)_{pq} C_{3qmn}. \tag{3.12}$$

4. Specific case: trabecular plates made of a homogeneous and isotropic material

Let the plate trabeculae be isotropic and homogeneous; then

$$C_{ijmn} = \mu\left(\delta_{mj}\delta_{ni} + \delta_{mi}\delta_{nj}\right) + \lambda\delta_{ij}\delta_{mn}.$$

From (3.11) we obtain the following form of the elasticity matrix:

(4.1)

$$\mathbf{C}^* = \begin{bmatrix} \frac{4\mu(\alpha+\beta)(\lambda+\mu)}{2\mu+\lambda} & \frac{2\alpha\lambda\mu}{2\mu+\lambda} & \frac{2\alpha\lambda\mu}{2\mu+\lambda} & 0 & 0 & 0 \\ \frac{2\beta\lambda\mu}{2\mu+\lambda} & \frac{4\mu(1+\beta)(\lambda+\mu)}{2\mu+\lambda} & \frac{2\lambda\mu}{2\mu+\lambda} & 0 & 0 & 0 \\ \frac{2\alpha\lambda\mu}{2\mu+\lambda} & \frac{2\lambda\mu}{2\mu+\lambda} & \frac{4\mu(1+\alpha)(\lambda+\mu)}{2\mu+\lambda} & 0 & 0 & 0 \\ 0 & 0 & 0 & 2\mu & 0 & 0 \\ 0 & 0 & 0 & 0 & 2\alpha\mu & 0 \\ 0 & 0 & 0 & 0 & 0 & 2\beta\mu \end{bmatrix}$$

Obviously, here Voigt's notation has been used, cf. [25].

Having in mind Fig. 6, the *physical* effective elasticity tensor, now denoted by $\mathbf{C}^{\text{eff}}$, is given by

(4.2)
$$\mathbf{C}^{\text{eff}} = \frac{v}{1+\alpha+\beta}\,\mathbf{C}^*,$$

where v is the volume fraction.

In the case of $\mathbf{C}^*$ given by Eq. (3.12) we have

$$\mathbf{C}^{\text{eff}} = \frac{vAB}{AB+B\alpha+A\beta}\,\mathbf{C}^*.$$

By $\mathbf{A}$ we denote the matrix inverse to $(\mathbf{C}^{\text{eff}})$, i.e. $\mathbf{A} = \left(\mathbf{C}^{\text{eff}}\right)^{-1}$. The technical elasticity constants are, cf. [16, 25]

(4.3)
$$E_1 = \frac{1}{A_{11}}, \qquad E_2 = \frac{1}{A_{22}}, \qquad E_3 = \frac{1}{A_{33}},$$

(4.4)
$$G_{12} = \frac{1}{2\,A_{66}}, \qquad G_{13} = \frac{1}{2\,A_{55}}, \qquad G_{23} = \frac{1}{2\,A_{44}},$$

(4.5)
$$\nu_{12} = -\frac{A_{12}}{A_{22}}, \qquad \nu_{21} = -\frac{A_{12}}{A_{11}}, \qquad \nu_{13} = -\frac{A_{13}}{A_{33}},$$
$$\nu_{31} = -\frac{A_{12}}{A_{11}}, \qquad \nu_{23} = -\frac{A_{23}}{A_{33}}, \qquad \nu_{32} = -\frac{A_{23}}{A_{22}}.$$

Let us pass now to the presentation of specific cases, which show the usefulness of the formulae (4.2) for the determination of macroscopic elastic moduli of a trabecular bone with a plate-like architecture. These particular cases are presented in the form of Tables 1, 2 and 3 and Figs. 7–9 below.

The third column of Table 1 provides technical constants calculated by using formulae (4.3) – (4.5). The following data, corresponding to the hydroxyapatite, cf. [9, 11], are assumed:

$$E = 114\,[\mathrm{GPa}], \qquad \nu = 0.27.$$

Then the Lamé coefficients are given by $\lambda = 52.69\,[\mathrm{GPa}]$, $\mu = 44.88\,[\mathrm{GPa}]$. The calculations have been performed for

$$\alpha = \frac{3}{4}, \quad \beta = \frac{1}{4}, \quad v = \frac{1}{5}.$$

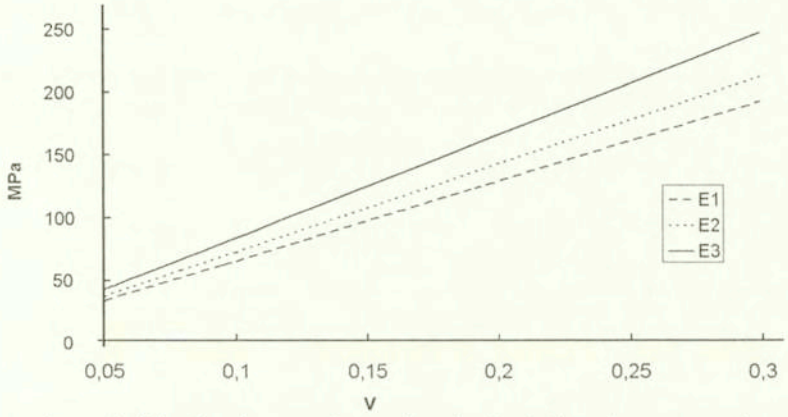

FIG. 7. Young's moduli in the three orthotropic principal directions versus bone volume fractions; $\alpha = 56/67$, $\beta = 73/134$; isotropic trabeculae with $E = 1$ [GPa], $\nu = 0.35$.

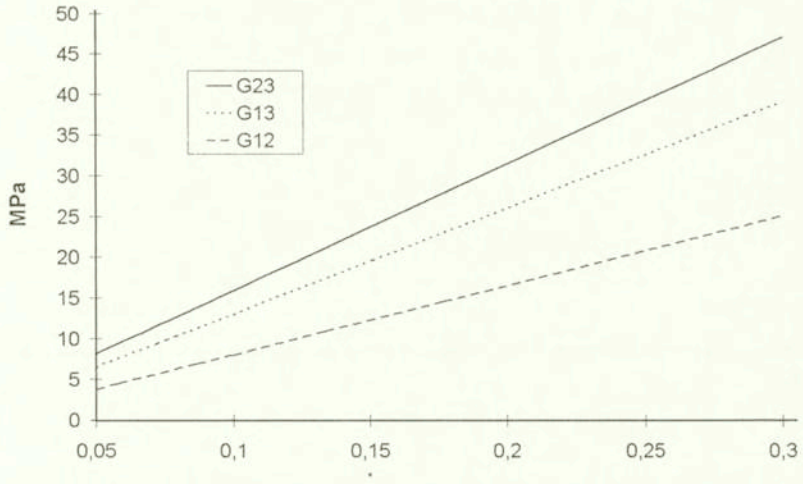

FIG. 8. Shear moduli in the three orthotropic principal directions versus bone volume fractions; $\alpha = 56/67$, $\beta = 73/134$; isotropic trabeculae with $E = 1$ [GPa], $\nu = 0.35$.

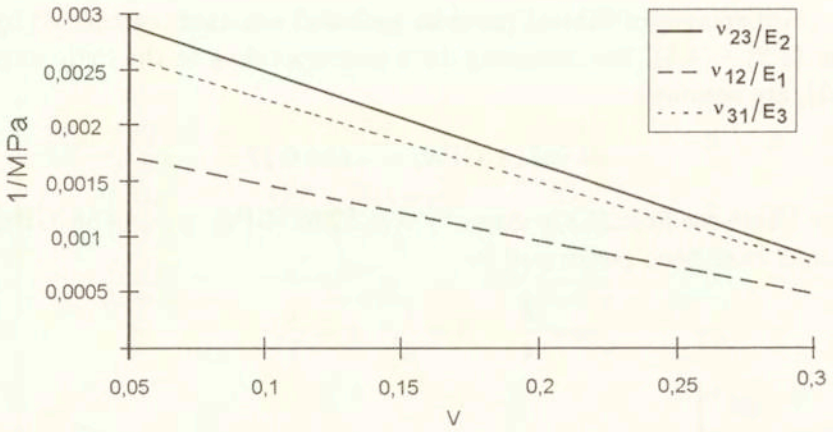

FIG. 9. Poisson's ratio divided by Young's moduli in the three orthotropic principal directions versus bone volume fraction; $\alpha = 56/67$, $\beta = 73/134$; isotropic trabeculae with $E = 1$ [GPa], $\nu = 0.35$.

The second column in Table 1 is taken from [16, Table 1].

Table 1. Technical constants

Technical constants (average)	human cortical bone	from (4.3) – (4.5) $E = 114$ [GPa], $\nu = 0.27$
E_1	11.7 (1.6) [GPa]	11.7 [GPa]
E_2	13.2 (1.8) [GPa]	14.4 [GPa]
E_3	19.8 (2.4) [GPa]	19.8 [GPa]
G_{12}	4.53 (0.37) [GPa]	1.1 [GPa]
G_{13}	5.61 (0.4) [GPa]	3.27 [GPa]
G_{23}	6.23 (0.48) [GPa]	4.36 [GPa]
ν_{12}	0.375 (0.095)	0.04
ν_{21}	0.416 (0.118)	0.03
ν_{23}	0.237 (0.083)	0.21
ν_{32}	0.346 (0.096)	0.15
ν_{13}	0.374 (0.108)	0.19
ν_{31}	0.234 (0.088)	0.11

Two further specific cases are summarized in the third and fourth column of Table 2. To calculate the moduli given in the third column of this table it was assumed that

$$\lambda = 52.69 \text{ [GPa]}, \qquad \mu = 44.88 \text{ [GPa]}, \qquad \alpha = \frac{56}{67},$$

$$\beta = \frac{73}{134}, \qquad v = 0.007.$$

Similarly, the moduli contained in the fourth column were calculated for the following data:

$$\lambda = 17.28 \text{ [GPa]}, \qquad \mu = 7.41 \text{ [GPa]}, \qquad \alpha = \frac{56}{67},$$

$$\beta = \frac{73}{134}, \qquad v = 0.043.$$

The second column of Table 2 is taken from [16, Table 1]. According to COWIN [9, Table 9], $E = 20$ [GPa] estimates the value of the elastic modulus of the wet human trabecula.

Table 2. Technical constants

Technical constants (average)	human cancellous bone (proximal tibia)	from (4.3) – (4.5) $E = 114$ [GPa], $\nu = 0.27$	from (4.3) – (4.5) $E = 20$ [GPa], $\nu = 0.35$
E_1	237 (63) [MPa]	496 [MPa]	545 [MPa]
E_2	309 (93) [MPa]	552 [MPa]	604 [Mpa]
E_3	823 (337) [MPa]	649 [MPa]	706 [MPa]
G_{12}	73 (0.37) [MPa]	73 [MPa]	73 [MPa]
G_{13}	112 (0.4) [MPa]	112 [MPa]	112 [MPa]
G_{23}	134 (0.48) [MPa]	134 [MPa]	134 [MPa]
ν_{12}	0.169 (0.304)	0.08	0.1
ν_{21}	0.209 (0.209)	0.07	0.09
ν_{23}	0.063 (0.217)	0.15	0.18
ν_{32}	0.245 (0.626)	0.11	0.14
ν_{13}	0.423 (0.356)	0.16	0.2
ν_{31}	0.145 (0.123)	0.14	0.17

We observe that the second column of Table 1 in [16], or the second column in our Table 1, present technical constants for specimens of human femoral cortical bone, where the 1-direction is radial, the 2-direction is circumferential and the 3-direction is longitudinal. The second column of Table 2 presents average technical constants for 9 specimens of human cancellous bone from the proximal tibia, where the 1-direction is anterior-posterior, the 2-direction is medial and 3-direction is logitudinal. In Tables 1 and 2 the numbers in parantheses stand for the standard deviations. The second column of Table 2 implies a possibility of appearance of negative values of Poisson's ratios. The plate-like architecture studied in the present paper precludes such possibility. Examples of cellular solids with negative Poisson's ratio are given in [23, 31]. Thus a natural question arises: can a trabecular bone, at a certain stage of human or animal life, behave like a cellular solid with negative Poisson's ratio? From the theoretical point of view, such possibility is obviously possible. The decisive answer, however, is to be expected from experimentalists.

We observe that according to Table 9 in [9], the value of E equal to 1.17 [GPa] characterises individual bovine trabeculae. This result was obtained by CHRISTENSEN (cf. [9]) using statistical data analysis. In Table 9 in [9] one also finds the following values of E [GPa] for individual trabeculae:

$E = 10.90 \pm 1.6$ (wet bovine femur, ultrasonic test method),

$E = 12.70 \pm 2$ (wet human femur, ultrasonic test method),

$E = 8.69 \pm 3.17$ (dry human distal femur, buckling test method),

$E = 5.3 \pm 2.6$ (dried human femur, experimental test method with finite element method).

According to Table 9 in [9], the estimates for the elastic modulus of the trabeculae of human cancellous bone vary from 1 to 20 [GPa]. Future research should be directed towards resolving this problem of great scatter of Young's moduli.

Table 3. Technical constants from (4.1) – (4.3)

Technical constants	$E = 1$ [GPa] $\nu = 0.35$ $\alpha = 0.836$ $\beta = 0.545$ $v = 0.1$	$E = 1$ [GPa] $\nu = 0.35$ $\alpha = 0.836$ $\beta = 0.545$ $v = 0.3$	$E = 5$ [GPa] $\nu = 0.3$ $\alpha = 0.9$ $\beta = 0.2$ $v = 0.2$	$E = 10$ [GPa] $\nu = 0.35$ $\alpha = 0.9$ $\beta = 0.2$ $v = 0,2$
E_1	0.0633 [GPa]	0.19 [GPa]	0.545 [GPa]	1.14 [GPa]
E_2	0.701 [GPa]	0.21 [GPa]	0.603 [GPa]	1.23 [GPa]
E_3	0.819 [GPa]	0.246 [GPa]	0.924 [GPa]	1.87 [GPa]
G_{23}	0.0156 [GPa]	0.0467 [GPa]	0.183 [GPa]	0.353 [GPa]
G_{13}	0.013 [GPa]	0.039 [GPa]	0.165 [GPa]	0.317 [GPa]
G_{12}	0.008 [GPa]	0.0254 [GPa]	0.0366 [GPa]	0.0705 [GPa]
ν_{23}	0.204	0.204	0.238	0.276
ν_{32}	0.175	0.175	0.156	0.182
ν_{12}	0.101	0.101	0.0164	0.0114
ν_{21}	0.0913	0.0913	0.0151	0.105
ν_{13}	0.184	0.184	0.232	0.269
ν_{31}	0.142	0.142	0.14	0.164

Figures 7–9 correspond to the data listed in the second and third column of Table 3.

Concluding remarks

The effective elastic moduli for a plate-like cellular solids were derived by using a mathematically rigorous homogenization approach. The solid considered is characterized by two small parameters: ϵ and η. The parameter η is related

to plates (trabeculae) thickness, cf. Fig. 6. The effective elasticity tensor is, in general, anisotropic. For $\alpha = \beta$ the macroscopic anisotropy is due to anisotropy of trabeculae. For $\alpha = \beta = 1$ and isotropic trabeculae the macroscopic elasticity tensor reveals the cubic symmetry (three material constants). If α is different from β and the trabeculae are isotropic, the macroscopic elasicity tensor is orthotropic. In Sec. 3 the basic cell was assumed to be given by (3.1). Unequal dimensions of this cell allong the three axes also influence the effective moduli.

In a separate paper we shall study the macroscopic behaviour of rod-like, trabecular bone. The first attempt was accomplished by us in [32].

Acknowledgement

The authors were supported by the State Committee for Scientific Research (Poland) through the grant No 8 T11F 018 12.

References

1. B. AOUBIZA, *Homogénéisation d'un composite multi-échelle: application à une modélisation numérique de l'os haversien compact*, Thèse, Université de Franche-Comté, 1991.
2. B. AOUBIZA and J.M. CROLET, A. MEUNIER, *On the mechanical characterization of compact bone structure using the homogenization theory*, J. Biomechanics, **29**, 1539–1547, 1996.
3. G.S. BEAUPRÉ and W.C. HAYES, *Finite element analysis of a three-dimensional opened-celled model for trabecular bone*, J. Biomech. Engng., **107**, 249–256, 1985.
4. M.P. BENDSØE, *Optimization of structural topology, shape, and material*, Springer-Verlag, Berlin 1995.
5. M.P. BENDSØE and N. KIKUCHI, *Generating optimal topologies in structural design using a homogenization method*, Comp. Mech. Appl. Mech. Enging. **71**, 192–224, 1988.
6. A. BENSOUSSAN, J.L. LIONS and G. PAPANICOULAOU, *Asymptotic analysis for periodic structures*, North-Holland, Amsterdam 1978.
7. D. CIORANESCU and J. SAINT JEAN PAULIN, *Reinforced and honey-comb structures*, J. Math. Pures Appl., **65**, 403–422, 1986.
8. D. CIORANESCU and J. SAINT JEANT PAULIN, *Asymptotic analysis of elastic wireworks*, Laboratoire d'analyse numérique, R89008, 1989.
9. S.C. COWIN, *The mechanical properties of cancellous bone* [in:] Bone mechanics, ed. by S.C. Cowin, pp. 129–157, CRC Press, Inc. Boca Raton, Florida 1989.
10. J.M. CROLET, *Homogenization: mathematical method applied to haversian cortical bone structure*, Proc. 1st World Congress of Biomechanics, 156–172, 1990.
11. J.M. CROLET, B. AOUBIZA and A. MEUNIER, *Compact bone: numerical simulation of mechanical characteristics*, J. Biomechanics, **26**, 677–687, 1993.
12. L.J. GIBSON, *The mechanical behaviour of cancellous bone*, J. Biomechanics, **18**, 317–328, 1985.
13. L.J. GIBSON and M.F. ASHBY, *Cellular solids: structure and properties*, Pergamon Press, New York 1988.

14. S.J. HOLLISTER, J.M. BRENNAN and N. KIKUCHI, *A homogenization sampling procedure for calculating trabecular bone effective stiffness and tissue level stress*, J. Biomechanics, **27**, 433–444, 1994.

15. S.J. HOLLISTER, D.P. FYHIRE, K.J. JEPSEN and S.A. GOLDSTEIN, *Application of homogenization theory to the study of trabecular bone mechanics*, J. Biomechanics, **24**, 825–839, 1991.

16. S. JEMIOŁO and J.J. TELEGA, *Fabric tensors in bone mechanics*, Engng. Trans., **46**, 3–26, 1998.

17. M. KASRA and M.D. GRYNPAS, *Static and dynamic finite element analyses of an idealized structural model of vertebral trabecular bone*, J. Biomech. Eng., **120**, 267–272, 1998.

18. R.V. KOHN and G. STRANG, *Optimal design and relaxation of variational problems*, I, II, III, Comm. Pure Appl. Math., **39**, 113–137, 139–182, 353–377, 1986.

19. T. LEWIŃSKI and J.J. TELEGA, Plates, Laminates and Shells: Asymptotic Analysis and Homogenization, World Scientific, in press.

20. G. LOWET, P. RÜEGSEGGER, H. WEINANS and A. MEUNIER [Eds], Bone Research in Biomechanics, IOS Press, Amsterdam 1997.

21. K.A. LURIE, A.V. FEDOROV and A.V. CHERKAEV, *Regularization of optimal design problems for bars and plates*, I and II, J. Opt. Theory Appl., **37**, 499–522, 523–543, 1982.

22. J. MCELHANEY, N. ALEM and V. ROBERTS, *A porous block model for cancellous bones*, ASME Publication No 70-WA/BHF-2, 1–9, 1970.

23. G.W. MILTON, *Composite materials with Poisson's ratio close to -1*, J. Mech. Phys. Solids, **40**, 1105–1137, 1992.

24. R. MÜLLER and P. RÜGSEGGER, *Micro-tomographic imaging for the nondestructive evaluation of trabecular bone architecture* [in:] Bone Research in Biomechanics, ed. by G. Lowet, P. Rüegsegger, H. Weinans and A. Meunier, pp. 61–79, IOS Press, Amsterdam 1997.

25. W. NOWACKI, *Elasticity theory* [in Polish], Państwowe Wydawnictwo Naukowe, Warszawa 1970.

26. W.M. PAYTEN, B. BEN-NISSAN and D.J. MERCER, *Optimal topology design using global self-organisational approach*, Int. J. Solids Structures, **35**, 219–237, 1998.

27. J.W. PUGH, R.M. ROSE and E.L. RADIN, *A structural model for the mechanical behavior of trabecular bone*, J. Biomechanics, **6**, 657–670, 1973.

28. E. SANCHEZ-PALENCIA, *Non- homogeneous media and vibration theory*, Springer-Verlag, Berlin 1980.

29. P.M. SUQUET, *Elements of homogenization theory for inelastic solid mechanics* [in:] Homogenization techniques for composite media, [Ed.] by E. Sanchez-Palencia and A. Zaoui, pp. 194–278, Springer-Verlag, Berlin 1985.

30. J.J. TELEGA and T. LEWIŃSKI, *A note on a saddle-point theorem in optimal compliance design*, [submitted.]

31. P.S. THEOCARIS, G.E. STAVROULAKISA and P.D. PANAGIOTOPOULOS, *Negative Poisson's ratio in composites with star-shaped inclusions: a numerical homogenization approach*, Arch. Appl. Mech., **67**, 274–286, 1997.

32. S. TOKARZEWSKI, A. GAŁKA and J.J. TELEGA, *Cancellous bone as a cellular solid: the determination of effective material properties* [Polish] [in:] Proc. of the Conf. on Biomechanics: Modelling, Computational Methods, Experiments and Biomedical Applications, [Ed.] by J. AWRAJCEWICZ, M. CIACH and M. KLEIBER, pp. 191–196, Technical University of Łódź 1998.

33. D. ULRICH, T. HILDEBRAND, B. van RIETBERGEN, R. MÜLLER and P. RÜEGSEGGER, *The quality of trabecular bone evaluated with micro-computed tomography, FEA and mechanical testing*, [in:] Bone research in biomechanics, [Ed.] by G. LOVET, P. RÜEGSEGGER, H. WEINANS and A. MEUNIER, pp. 97–112, IOS Press, Amsterdam 1997.

34. J.L. WILLIAMS and J.L. LEWIS, *Properties and anisotropic model of cancellous bone from the proximal tibia epiphysis*, J. Biomech. Engng., **104**, 50–56, 1982.

35. P.K. ZYSSET, R.W. GOULET and S.J. HOLLISTER, *A global relationship between trabecular bone morphology and homogenized elasic properties*, J. Biomech. Eng., **120**, 640–646, 1998.

Received January 14, 1999; revised version March 26, 1999.